catalysts

MDPI

Article

Synergy between Sulfonic Functions and Ru Nanoparticles Supported on Activated Carbon for the Valorization of Cellulose into Sorbitol

Samuel Carlier [1], Walid Baaziz [2], Ovidiu Ersen [2] and Sophie Hermans [1,*]

[1] IMCN Institute, Université Catholique de Louvain, Place L. Pasteur 1, 1348 Louvain-la-Neuve, Belgium; samuel.carlier@uclouvain.be
[2] Institut de Physique et de Chimie des Matériaux de Strasbourg, CNRS-UMR7504, 23 rue du Loess, CEDEX 2 BP 43, 67034 Strasbourg, France; walid.baaziz@ipcms.unistra.fr (W.B.); ovidiu.ersen@ipcms.unistra.fr (O.E.)
* Correspondence: sophie.hermans@uclouvain.be

Abstract: The production of sorbitol from biomass, and especially from its cellulosic component, has been studied as a sustainable method for producing platform molecules. Because it requires two steps, namely, hydrolysis and hydrogenation, bifunctional materials are required as catalysts for this transformation. This study reports a bifunctional catalyst composed of sulfonic functions grafted onto a carbon support for the hydrolysis step and RuO_2 nanoparticles for the hydrogenation step. As sulfur can easily poison Ru, synthetic optimization is necessary to obtain an efficient bifunctional catalyst that surpasses a mere Ru/C catalyst. Kinetic studies highlight the better activity of the bifunctional catalysts compared to the reference monofunctional catalysts. Besides being active in hydrolysis reactions, sulfonic functions also have a role in avoiding the degradation of the sorbitol produced. The recyclability of the bifunctional catalyst is also superior to that of the monofunctional one.

Keywords: biomass; cellulose; sorbitol; bifunctional catalyst; sulfonic; ruthenium; carbon; hydrogenolysis

Citation: Carlier, S.; Baaziz, W.; Ersen, O.; Hermans, S. Synergy between Sulfonic Functions and Ru Nanoparticles Supported on Activated Carbon for the Valorization of Cellulose into Sorbitol. *Catalysts* **2023**, *13*, 963. https://doi.org/10.3390/catal13060963

Academic Editors: Roger A. Sheldon, Dmitry Yu. Murzin, Yulong Wu, Reinout Meijboom and Georgios Papadogianakis

Received: 31 March 2023
Revised: 15 May 2023
Accepted: 26 May 2023
Published: 1 June 2023

1. Introduction

Lignocellulose is the dominant non-edible biomass resource in our environment. Its valorization into fine chemicals is one of the most important challenges to finding renewable and sustainable alternatives to fossil fuels [1–4]. It is composed of lignin (10–30%), hemi-cellulose (15–40%) and cellulose (30–65%) [5]. Lignin is a phenylpropanoid polymer linked randomly. Hemi-cellulose is a non-linear polymer of pentose, hexoses and sugar acids. Cellulose is a linear polymer of glucose units linked by β-1,4-glycosidic bonds. The treatment of lignocellulosic biomass can produce many useful molecules, such as glucose, 5-hydroxymethylfurfural, sorbitol, aromatic alcohols or aldehydes, furfural, xylitol, etc. [4,6–9]. The transformation of cellulose into sorbitol has been extensively studied because sorbitol is a platform molecule of interest. It can be used as a sweetener or an excipient in the food and cosmetics industries [10,11]. However, this transformation is very challenging. Cellulose hydrolysis is the trickiest part because cellulose has a microcrystalline structure. Intra- and intermolecular as well as inter-sheet hydrogen bonds make it insoluble in almost all solvents, especially water [12]. Assistance in reducing the crystallinity of cellulose and breaking it into oligomers is often used in cellulose transformation processes. Ionic liquids can dissolve cellulose by preventing intermolecular hydrogen bonds, but these liquids are very expensive and toxic [13]. Supercritical water is also used to partially dissolve cellulose [14]. Ball milling can reduce mechanical cellulose crystallinity [15,16]. Microwave irradiation is also a common method to depolymerize cellulose via the in situ generation of heat [4,17]. Nowadays, mineral acids such as HCl

or H_2SO_4 are used industrially as homogeneous catalysts to depolymerize cellulose. This method generates a lot of waste, which has to be disposed of and damages the reaction vessels [18,19]. The use of enzymes, such as cellulases, is a very efficient alternative to process cellulose [20]. Even if this method is efficient and more selective, it is very costly, the enzymes cannot support high temperatures and the recyclability is very low [21]. These methods are needed to break cellulose into smaller oligomers that will be more soluble in water in order to be able to process them further. The smallest unit retaining the glycosidic bond is cellobiose, with only two glucose units (Scheme 1), and can serve as a model compound in these studies.

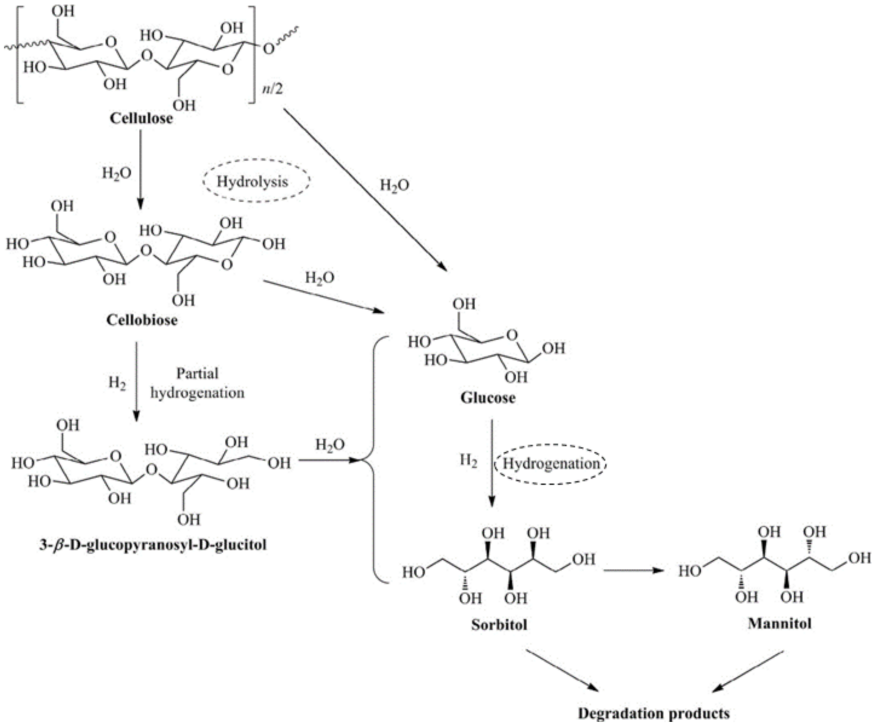

Scheme 1. Reaction pathways for the transformation of cellulose into sorbitol. Reprinted from ref. [4] with permission from Elsevier.

In complement to the use of pre-treatment methods, acidic heterogeneous catalysts have been extensively studied in biomass valorization. Even though they will show less activity, they will display stability, recyclability and robustness. Various acidic heterogeneous catalysts have been investigated, such as Amberlyst-15 resin [22], hydrotalcites [23], zeolites [24], functionalized carbon materials [25,26] and so on. Glucose arising from cellulose depolymerization can then be hydrogenated into sorbitol. Industrially, this step is catalyzed by using Ni-Raney. However, many studies have tried to improve this transformation by using noble metals, such as Ru [27] or even the more expensive Pt [28]. Nowadays, the challenge is to directly transform cellulose into sorbitol using a bifunctional catalyst that will display acidic functions and Ru active sites. Different types of supports have been investigated in such contexts: MCM-48 [29], ZSM-5 zeolites [30], modified SiO_2 [31] and metal–organic framework (MOF) [32]. Carbon materials have been functionalized with acidic functions, such as COOH or SO_3H, and have supported Ru nanoparticles [33,34].

The reaction pathways from cellulose to sorbitol are shown in Scheme 1. It has to be pointed out that by using bifunctional catalysts, it is possible to first hydrogenate cellobiose into 3-β-D-glucopyranosyl-D-glucitol (cellobitol) and then hydrolyze it into glucose and sorbitol or, as discussed above, to first hydrolyze and then hydrogenate. It has been shown that this alternative pathway (with hydrogenation first) is faster than hydrolyzing first [35]. Moreover, the hydrogenation of glucose just after its release from cellulose decreases the

amount of degradation products [36]. Therefore, the one-pot production of sorbitol from cellulose through the action of an efficient bifunctional catalyst would be a milestone in biomass processing.

The purpose of the present contribution is to use sulfonic functions jointly with Ru nanoparticles to obtain a bifunctional carbon-supported catalyst that can transform cellobiose and, more importantly, cellulose directly into sorbitol. Sulfonic functions will be grafted covalently by using an organic reaction on the carbon surface to produce a highly acidic support. An optimal balance between the amount of sulfur and the amount of Ru will be targeted to avoid poisoning Ru and still display the best possible catalyst activity. These bifunctional catalysts will be first tested on cellobiose, as a water-soluble model for cellulose, allowing the study of its hydrogenolysis into sorbitol without the need for assistance systems to increase solubility. Eventually, the transformation of cellulose into sorbitol will be assessed with the best bifunctional catalysts to highlight the synergetic effects between the two types of active sites and benchmark our new materials.

2. Results and Discussion

2.1. Cellobiose Transformation into Sorbitol

The synthesis of bifunctional catalysts with both sulfonic functions and Ru is a challenge because it is known that sulfur, especially under high-pressure and high-temperature catalytic testing conditions, can strongly poison noble metals [37], especially Ru [38]. Therefore, it was decided to first functionalize the carbon support with sulfonic functions before adding the Ru nanoparticles to limit the poisoning of the active metal phase. The method employed for carbon functionalization has already been discussed in another study [26] and is described in the experimental section. To keep the integrity of the sulfonic functions, a neutral method to add the RuO_2 nanoparticles was used, namely, the adsorption of preformed colloidal RuO_2 suspension. The Ru is reduced in situ by using H_2 during the reaction. Catalytic tests were carried out with monofunctional, either with sulfonic functions alone or with only Ru nanoparticles, and bifunctional catalysts (Table 1).

Table 1. Hydrogenolysis of cellobiose with monofunctional and bifunctional catalysts. Cellobiose conversion; glucose, cellobitol and sorbitol selectivities; sorbitol yield (150 °C, 30 bar of H_2, 2 h, 150 mg of catalyst with 1 wt.% of Ru). The estimated confidence interval for cellobiose conversion and selectivities is 3%.

Catalyst	Cellobiose Conversion (%)	Glucose Selectivity (%)	Cellobitol Selectivity (%)	Sorbitol Selectivity (%)	Sorbitol Yield (%)
RuO_2/AC	100	0	59	29	29
SO_3H/AC	61	86	0	0	0
RuO_2–SO_3H/AC	65	84	0	2	1
RuO_2/AC and SO_3H/AC [1]	84	81	0	2	2

[1] Mechanical mix between the two monofunctional catalysts.

The hydrogenation pathway is favored with the RuO_2/AC catalyst, which essentially provided cellobitol and sorbitol. The SO_3H/AC acid monofunctional catalyst yielded a high amount of glucose, as expected in the absence of Ru to catalyze the hydrogenation. Unfortunately, with the corresponding bifunctional catalyst, prepared in exactly the same way, with both SO_3H and Ru on the support, sorbitol was not obtained. However, the results were very similar to those obtained with the acidic catalyst without Ru. This means that all Ru is poisoned by the sulfur of the sulfonic functions, even if the metal component was introduced in the second position. A test with the two monofunctional catalysts mechanically mixed was carried out, and the result was still similar to SO_3H/AC. Even if the sulfonic functions were not on the same support, they managed to poison the Ru. Sulfonic functions are likely leaching during the reaction and can poison Ru on other catalyst grains.

In order to enhance bifunctional catalyst activity, several parameters were studied to optimize the ratio between sulfur and ruthenium and avoid this poisoning effect. To control the amount of sulfur for the preparation of bifunctional catalysts, the modulation of the sulfonic functions grafted onto the carbon supports by heat treatment (under an N_2 atmosphere) was investigated (Table 2). By increasing the heat treatment temperature, a decrease in the O and S surface amounts was observed. While the acidity (determined by Boehm titration) did not decrease at 200 °C, it was lower after treatment at 300 °C and 400 °C. This indicates that the sulfonic functions present in the carbon materials are logically more abstracted when the temperature of the treatment increases. It has been shown by TPD–MS that these grafted sulfonic acid groups do not start to decompose at all before 200 °C, with the main decomposition temperature above 300 °C [26].

Table 2. Oxygen and sulfur contents determined by using XPS and acidity from Boehm titration of the acidic catalysts without heat treatment and heat-treated at 200 °C, 300 °C and 400 °C.

Catalyst	O (at. %)	S (at. %)	Acidity (mmol/100 g)
AC	4.3	0	42
SO_3H/AC	12.95	3.66	145
SO_3H 200 °C/AC	10.33	2.96	146
SO_3H 300 °C/AC	7.53	1.51	115
SO_3H 400 °C/AC	2.88	0.75 [1]	69

[1] Total S at. % (addition of sulfonic peak and thiol peak).

These new catalysts with varying acidities were assessed in the hydrolysis of cellobiose into glucose under a nitrogen atmosphere (Table 3). As expected, the activity of the catalysts decreased with the applied heat treatment temperature. The low selectivity into glucose obtained for the catalysts heated at 300 °C and 400 °C is the same selectivity obtained when the test was conducted without any catalyst (blank test). The remaining sulfonic functions were no longer useful after these heat treatments. This confirms that sulfonic functions are indeed present in lower amounts when the temperature of the heat treatment is increased. Moreover, this is consistent with our previous work, which showed that a minimum amount of SO_3H is needed to trigger the hydrolysis of cellobiose [26]. It was also shown that the heat treatments at 200 °C and 300 °C did not modify the nature of the sulfonic functions. Indeed, XPS analyses showed that the sulfur peak did not shift (S1 in the Supplementary Materials). However, the heat treatment at 400 °C formed thiols (at 164 eV) on the support surface in addition to the remaining sulfonic functions (at 168.5 eV) (S1 in the Supplementary Materials).

Table 3. Hydrolysis of cellobiose. Cellobiose conversion, glucose selectivity and yield (150 °C, N_2, 2 h, 150 mg of catalyst) obtained with acid catalysts heat-treated at different temperatures. The estimated confidence interval for cellobiose conversion and selectivities is 3%.

Catalyst	Cellobiose Conversion (%)	Glucose Selectivity (%)	Glucose Yield (%)
Blank	22	43	9
SO_3H/AC	88	83	73
SO_3H 200 °C/AC	47	79	37
SO_3H 300 °C/AC	22	39	9
SO_3H 400 °C/AC	22	35	8

These supports, possessing different amounts of sulfonic functions, were then used to prepare a new set of bifunctional catalysts by depositing RuO_2 nanoparticles. The hydrogenolysis of cellobiose was tested for 2 h with these materials to investigate the impact of the Ru/S ratio on the performance of the catalysts (Table 4).

Table 4. Hydrogenolysis of cellobiose with bifunctional catalysts possessing different amounts of sulfonic functions. Cellobiose conversion; glucose, cellobitol and sorbitol selectivities; sorbitol yield (150 °C, 30 bar of H_2, 2 h, 150 mg of catalyst with 1 wt.% of Ru). The estimated confidence interval for cellobiose conversion and selectivities is 3%.

Catalyst	Cellobiose Conversion (%)	Glucose Selectivity (%)	Cellobitol Selectivity (%)	Sorbitol Selectivity (%)	Sorbitol Yield (%)
RuO_2–SO_3H 200 °C/AC	66	84	0	1	1
RuO_2–SO_3H 300 °C/AC	55	45	37	4	2
RuO_2–SO_3H 400 °C/AC	51	17	55	13	7

The results show that the pathway of the reaction is different depending on the ratio between Ru and the sulfonic functions. When the functionalized support is treated at 200 °C, sulfonic groups are still present in high amounts, poisoning the Ru. Therefore, the hydrolysis of cellobiose into glucose is the main reaction, and sorbitol is not produced. After treatment at 300 °C, sulfonic functions are degraded partially (as confirmed by the XPS results displayed in S3 section in the Supplementary Materials), and both pathways are followed in parallel. Glucose (the hydrolysis product) and cellobitol (the hydrogenation product) are produced simultaneously, while sorbitol production remains really low due to the very short testing duration. The material pre-heated at 400 °C produced more sorbitol, while glucose selectivity was rather low compared to cellobitol selectivity. This means that, in this case, the hydrogenation pathway is the major one. All these observations were confirmed with kinetic studies with each of these catalysts (S2 section in the Supplementary Materials). After 24 h, it was observed that the bifunctional catalysts pre-heated at 300 °C and 400 °C produced sorbitol, while the lower-temperature-treated bifunctional catalyst barely managed to form some of it. The diminution in sulfonic function amounts allows the Ru to be less poisoned, and the resulting bifunctional catalysts can produce sorbitol. However, the sorbitol production was not better than a monofunctional catalyst with only Ru deposited on the unmodified carbon support. Therefore, other ways of enhancing sorbitol productivity were investigated.

In order to study a different method that could prevent the poisoning of Ru by sulfur, consecutive reactions with both monofunctional catalysts were carried out (Table 5). Cellobiose conversion and sorbitol yield are always given with respect to the first starting compound, even in the case of consecutive reactions. First, hydrogenation using the RuO_2/AC catalyst was carried out, and then, the solid was filtered out. Consecutively, the SO_3H/AC catalyst was added to catalyze the hydrolysis. By doing so, a sorbitol yield of 46% in 2 h was obtained, which was, by far, better than with any other catalyst tested so far. It is important to highlight the fact that when cellobitol is hydrolyzed, it provides one equivalent of glucose and one equivalent of sorbitol. When staged in this order, the two reactions cannot provide 100% of sorbitol because the glucose produced needs to be further hydrogenated. If the two consecutive reactions are performed in the opposite order (first hydrolysis and then hydrogenation), it was noticed that the sorbitol yield was dramatically lower (11%). This result can be explained by the fact that during hydrolysis some sulfonic functions will leach and go into solution. Indeed this was confirmed as the pH went down from 5 to 3 after the hydrolysis step. Then, when the RuO_2/AC was added for the second reaction, it was poisoned by the sulfur compounds present within the solution, decreasing the activity of Ru.

Table 5. Consecutive reactions with SO_3H/AC without and with a pre-treatment and RuO_2/AC catalysts. Cellobiose conversion; glucose, cellobitol and sorbitol selectivities; sorbitol yield (150 °C, 30 bar of H_2 or autogenic pressure of N_2, 2 h, 150 mg of catalyst with 1 wt.% of Ru). The estimated confidence interval for cellobiose conversion and selectivities is 3%.

Catalyst	Cellobiose Conversion (%)	Glucose Selectivity (%)	Cellobitol Selectivity (%)	Sorbitol Selectivity (%)	Sorbitol Yield (%)
RuO_2/AC for 2 h under H_2	100	0	52	29	29
SO_3H/AC for 2 h under N_2	100	6	30	46	46
SO_3H/AC for 2 h under N_2	62	88	0	0	0
RuO_2/AC for 2 h under H_2	88	36	32	13	11
Pre-treated SO_3H/AC for 2 h under N_2	51	98	0	0	0
RuO_2/AC for 2 h under H_2	100	10	27	37	37

As sulfonic functions can leach and poison Ru nanoparticles, a pre-treatment under the same conditions as the catalytic tests was conducted to remove all labile functions and keep solely the sulfonic groups well grafted onto the carbon support. This type of pre-treatment has been shown in previous work to provide 116 mmol/100 g of acidity, with good results for the hydrolysis of cellobiose into glucose (98% selectivity toward glucose) [26]. XPS data of the pre-treated SO_3H/AC can be found in the Supplementary Materials (S3 section). Two consecutive reactions were carried out with first the pre-treated SO_3H/AC catalyst and then with the RuO_2/AC catalyst.

The sorbitol yield at the end of the two consecutive reactions was significantly higher when the SO_3H/AC was pre-treated in this way (Table 5, bottom). This shows, indeed, that the pre-treatment can lower the quantity of labile sulfonic functions that can poison the Ru nanoparticles. However, there is still a portion of sulfonic functions that inhibit the Ru. Indeed, the obtained yield is not as good as when the two consecutive reactions were carried out in the opposite order. Nevertheless, this pre-treatment on the sulfonic functions was used to prepare new bifunctional catalysts that would suffer less from the poisoning of Ru. This time the Ru/S ratio was studied by varying the amount of Ru. New catalysts with 1 wt.%, 3 wt.% and 5 wt.% of Ru were synthesized using pre-treated SO_3H/AC as the support. They were assessed as catalysts in comparison with corresponding mono- and bifunctional catalysts without pre-treatment (Table 6) in the one-pot direct hydrogenolysis of cellobiose into sorbitol.

The results obtained with the bifunctional catalyst with 1 wt.% of Ru are similar to the bifunctional catalyst prepared without any pre-treatment of the sulfonic functions. Indeed, even if the amount of sulfonic functions decreases with the pre-treatment, it is still enough to totally inhibit the Ru active phase. For the monofunctional catalyst with 3 wt.% of Ru, it can be observed that the sorbitol yield was the same that the monofunctional catalyst with 1 wt.%. Nevertheless, if the quantity of cellobitol is lower, the sorbitol yield should be higher. This means that sorbitol seems to react further or suffer from degradation. The bifunctional catalyst with 3 wt.% of Ru is more active than the one with 1 wt.%. Interestingly, the apparition of cellobitol and sorbitol in the products can be seen. This indicates that both pathways (as seen in Scheme 1) are followed and both Ru nanoparticles and sulfonic functions are active at the same time. However, the sorbitol yield was still not higher than with the monofunctional catalyst. It can also be observed that the bifunctional catalyst with 3 wt.% of Ru without the pre-treatment of sulfonic functions displays a lower yield of sorbitol. The monofunctional catalyst with 5 wt.% of Ru provides a higher yield of sorbitol, which was expected as the Ru quantity increased. Finally, the bifunctional catalyst with

5 wt.% provides the best results. Indeed, the sorbitol yield reached 53% in 2 h, indicating that a synergy between the two active sites occurred with this ratio between Ru and SO_3H functions (10 Ru atoms for 1 S atom based on XPS analysis). The sorbitol yield decreased drastically to 13% when the SO_3H functions were not pre-treated. This highlights the importance of this pre-treatment in order to have an efficient bifunctional catalyst.

Table 6. Hydrogenolysis of cellobiose with monofunctional and bifunctional catalysts with different Ru weight percentages and pre-treated supports. Cellobiose conversion; glucose, cellobitol and sorbitol selectivities; sorbitol yield (150 °C, 30 bar of H_2, 2 h, 150 mg of catalyst). The estimated confidence interval for cellobiose conversion and selectivities is 3%.

Catalyst	Cellobiose Conversion (%)	Glucose Selectivity (%)	Cellobitol Selectivity (%)	Sorbitol Selectivity (%)	Sorbitol Yield (%)
RuO_2 (1%)/AC	100	0	59	29	29
RuO_2 (1%)–pre-treated SO_3H/AC	61	80	0	2	1
RuO_2 (1%)–SO_3H/AC	65	84	0	2	1
RuO_2 (3%)/AC	100	4	34	30	30
RuO_2 (3%)–pre-treated SO_3H/AC	85	26	40	22	19
RuO_2 (3%)–SO_3H/AC	77	43	36	11	8
RuO_2 (5%)/AC	100	3	19	43	43
RuO_2 (5%)–pre-treated SO_3H/AC	100	6	29	53	53
RuO_2 (5%)–SO_3H/AC	76	29	44	17	13

Kinetic studies were carried out on the monofunctional and bifunctional catalysts with 5 wt.% of Ru to highlight the differences between them (Figure 1). It can be observed that the bifunctional catalyst provided a higher sorbitol yield than the monofunctional catalyst during all investigated timeframes. The conversion of cellobiose and sorbitol selectivity/yield are presented in the Supplementary Materials (S4 section). The sorbitol yield was the same after 6 h and after 24 for the monofunctional catalyst, whereas cellobitol decreased. This confirms our assumption that sorbitol reacts further during the reaction. This did not happen with the bifunctional catalyst. The combination of SO_3H functions and Ru nanoparticles in this optimized ratio stabilizes the sorbitol, thereby preventing it from reacting further or degrading. This effect has already been reported in the literature [31]. This explains the higher yield of sorbitol at the end of the reaction. The bifunctional catalyst is not more active than the monofunctional catalyst; indeed, the conversion is lower at the beginning of the reaction with the RuO_2-pre-treated SO_3H/AC catalyst, but it stabilizes the sorbitol, which provides all in all a much higher yield. This effect is striking after 24 h of reaction, with a yield of 11% for the monofunctional catalyst compared to 79% for the bifunctional catalyst.

The degradation of sorbitol with the RuO_2/AC and bifunctional catalyst was studied. Sorbitol (the product of the reaction), rather than cellobiose, was placed in the presence of the two catalysts under the same conditions as in the previous tests. The results show that RuO_2/AC transformed 50% of the sorbitol under these conditions, while the bifunctional catalyst transformed only 7% of the sorbitol within 2 h. The presence of SO_3H functions highly stabilizes the sorbitol molecule and prevents it from degradation. Unfortunately, the products formed by sorbitol degradation could not be identified. A list of molecules that were injected in HPLC and that can be ruled out from possible side products can be found in the Supplementary Materials (S5 section).

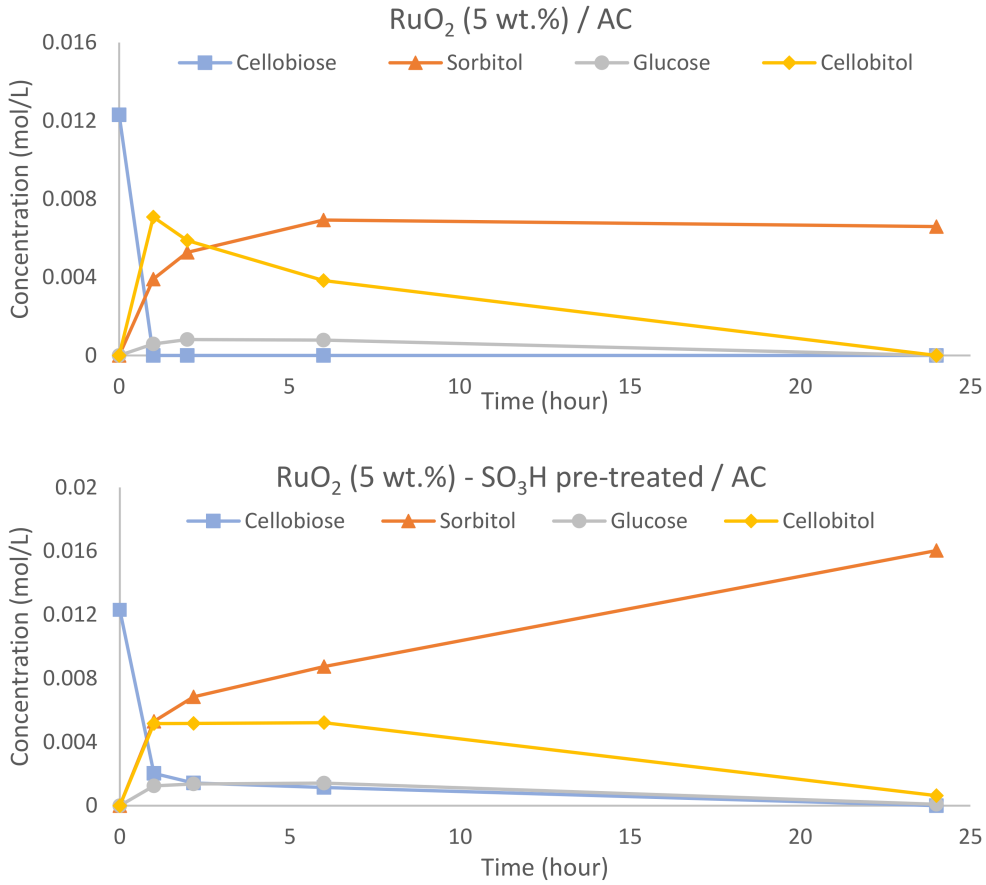

Figure 1. Kinetic curves for the hydrogenolysis of cellobiose into sorbitol (testing conditions: 150 °C, 30 bar of H_2, 24 h, 150 mg of catalyst); the lines connecting experimental points are only a visual aid and do not correspond to any mathematical model.

To further optimize the Ru/S ratio, modification of the sulfur amount with thermal pre-treatment was investigated with 5 wt.% of Ru loading (Table 7). The bifunctional catalyst with sulfonic functions treated at 200 °C provided the same amount of glucose as sorbitol. This means that there were still too many sulfonic groups and that the Ru nanoparticles were poisoned. When the sulfonic functions were treated at 300 °C, the results were the same as when the sulfonic functions were pre-treated in water. The bifunctional catalyst is better than the reference RuO_2/AC, showing synergy between the two types of active sites. After heat treatment at 400 °C, the bifunctional material displayed a lower activity. Indeed, the sulfonic functions were more degraded, leading to more active Ru nanoparticles and sorbitol degradation. The synergy between the two active sites was no longer observable.

Eventually, the recyclability of both the monofunctional and bifunctional catalysts was assessed. Five catalytic tests were carried out for each catalyst (Figure 2). Both catalysts suffered from deactivation after the first run, but the impact was less important on the bifunctional catalyst than on the monofunctional catalyst. The activity was then stable over the next runs. TOC analysis of the solution after catalytic tests showed that the carbon balance was respected.

Table 7. Hydrogenolysis of cellobiose with bifunctional catalysts possessing sulfonic functions treated at different temperatures. Cellobiose conversion; glucose, cellobitol and sorbitol selectivity; sorbitol yield (150 °C, 30 bar of H_2, 2 h, 150 mg of catalyst with 5 wt.% of Ru). The estimated confidence interval for cellobiose conversion and selectivities is 3%.

Catalyst	Cellobiose Conversion (%)	Glucose Selectivity (%)	Cellobitol Selectivity (%)	Sorbitol Selectivity (%)	Sorbitol Yield (%)
RuO_2 (5 wt.%)–SO_3H 200 °C/AC	100	26	31	21	21
RuO_2 (5 wt.%)–SO_3H 300 °C/AC	100	0	40	47	47
RuO_2 (5 wt.%)–SO_3H 400 °C/AC	100	0	47	38	38

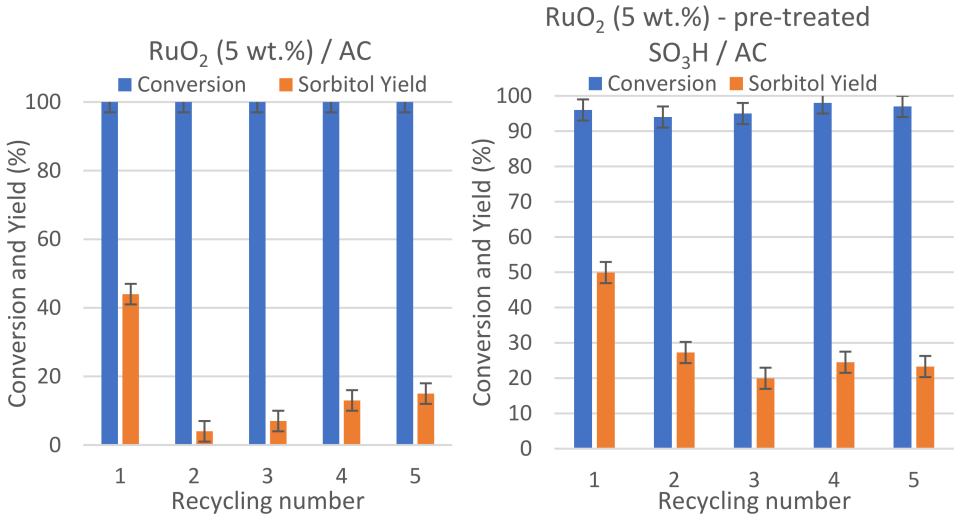

Figure 2. Recycling tests with monofunctional RuO_2/AC and bifunctional RuO_2-pre-treated SO_3H/AC catalysts.

XPS characterizations were performed on the monofunctional and bifunctional catalysts before and after the catalytic tests. The results are presented in Table 8, while the XPS narrow scans can be found in the Supplementary Materials (S6 section). As the Ru amount in the catalysts is important, Ru_{3d} has to be subtracted from the carbon C_{1s} signal; otherwise, the carbon will be overestimated, leading to erroneous percentages for other elements. Ru_{3p} was also analyzed to confirm the Ru_{3d} data, but only the Ru_{3d} results will be displayed in this article in order to quantify the Ru surface at. % and Ru oxidation states. The Ru_{3d} (IV) amount was higher for the bifunctional catalyst than the monofunctional one before the catalytic test. The same statement can be made for the catalysts with 3 wt.% of Ru (S7 section in the Supplementary Materials). The in situ activation of Ru in the reactor was confirmed by these analyses. Indeed, as expected, the Ru(0) amount was drastically increased after the catalytic tests. It is known that Ru can be reduced during XPS analyses, explaining the small amount of Ru(0) in the catalysts before the tests. It should be noted that not all Ru(IV) was reduced during the catalytic tests. The main assumption based on the XPS results is that the core of the nanoparticles was not reduced, and only the surface became Ru(0), giving core-shell structures. When superposing the Ru_{3p} regions of the catalysts before and after multiple runs (corresponding to Figure 2), it is obvious that Ru was reduced during the catalytic tests (see Figure 9 in the Supplementary Materials).

Table 8. Atomic percentage of C_{1s} and Ru_{3d} from XPS analyses for monofunctional and bifunctional catalysts before and after five catalytic tests.

Catalyst	C_{1s} (at. %)	S_{2p} (at. %) (SO_3H Functions)	O_{1s} (at. %)	Ru_{3d} (IV) (at. %)	Ru_{3d} (0) (at. %)
RuO_2 (5%)/AC	62.5	N/A	25.9	7.1	1.7
RuO_2 (5%)–pre-treated SO_3H/AC	52.7	0.9	34.3	8.3	1.5
RuO_2 (5%)/AC after 5 runs	73.9	N/A	18.2	1.9	5.3
RuO_2 (5%)–pre-treated SO_3H/AC after 5 runs	71.0	2.1	21.4	1.2	3.4

The amount of S, the position of the S_{2p} peak and the increase in O after sulfonic functionalization corroborate the success of the reaction, as presented above. These results were confirmed by the bulk analysis of the bifunctional catalyst (before catalytic reaction). This analysis revealed 3.7 wt.% of Ru and almost 3 wt.% of S. The nominal value of 5 wt.% of Ru was not reached due to the fact that Ru forms refractory oxides during sample preparation for ICP analysis, so this analysis underestimates the metal content. The S amount is quite important, explaining the significant Ru poisoning.

XRD analyses were also conducted on these catalysts (Figure 3). The wide peak between 12° and 28° comes from the carbon support (AC) [39]. The sharp peak at ~27 ° is probably due to graphitic C or S but cannot be ascribed to Ru species. The Ru peak is around 44° [40]. This is very low for the catalysts before the reaction because it is essentially RuO_2. After the reaction, Ru was reduced and the Ru peak increased because Ru(0) is crystalline in the case of the monofunctional catalyst, but surprisingly not for the bifunctional catalyst. It seems that the presence of sulfonic functions interferes with the crystallinity of the Ru(0) domains and decreases it.

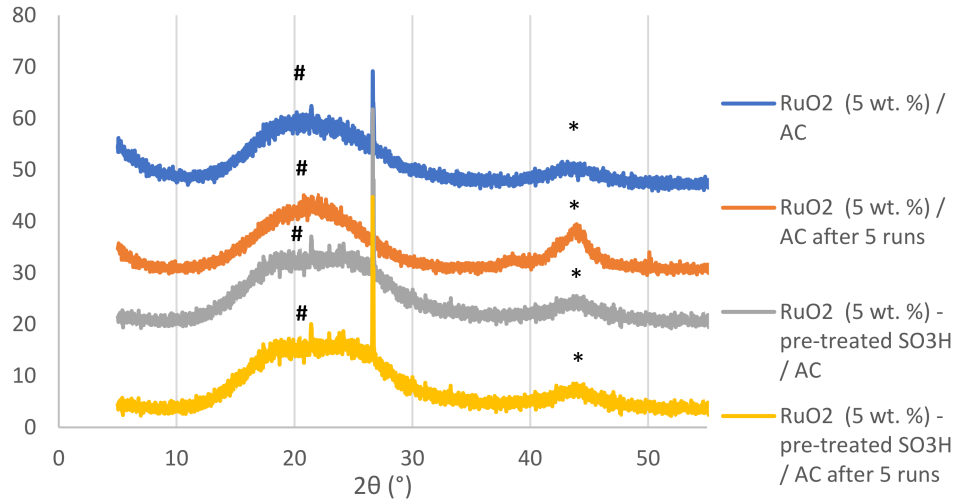

Figure 3. XRD analyses of monofunctional and bifunctional catalysts before and after catalytic tests. Asterisks denote peaks attributed to Ru metal phases and # denotes carbon phase.

HR-TEM images were obtained for the four catalysts (Figure 4). The RuO_2 nanoparticle preparation method can be adapted to control their sizes, and a nanoparticle size of 1–2 nm was targeted here [41]. The images show that the RuO_2 nanoparticles have a mean size of around 1 nm, as expected. The distribution and size of the nanoparticles are the same without or with sulfonic functions (see Figure 4a,b for comparison). EDX mapping analyses were performed and confirmed the good dispersion of Ru on the carbon support (S8 section in the Supplementary Materials). When the support was functionalized by the sulfonic functions, sulfur was found everywhere on the carbon support. There was no specific

area that could be identified where Ru and S were more present together. The catalysts recovered after the catalytic reaction (five runs) were also analyzed by using HR-TEM (Figure 4c,d) and EDX (S8 section in the Supplementary Materials). The TEM images show that the Ru nanoparticles were still well dispersed on the support. However, due to the high temperature during the reaction, a small increase in nanoparticle size could be observed after catalyst recovery, but the nanoparticle size was still between 1 and 2 nm. The presence of sulfur all over the support for the bifunctional catalyst after five runs was also confirmed by EDX analyses.

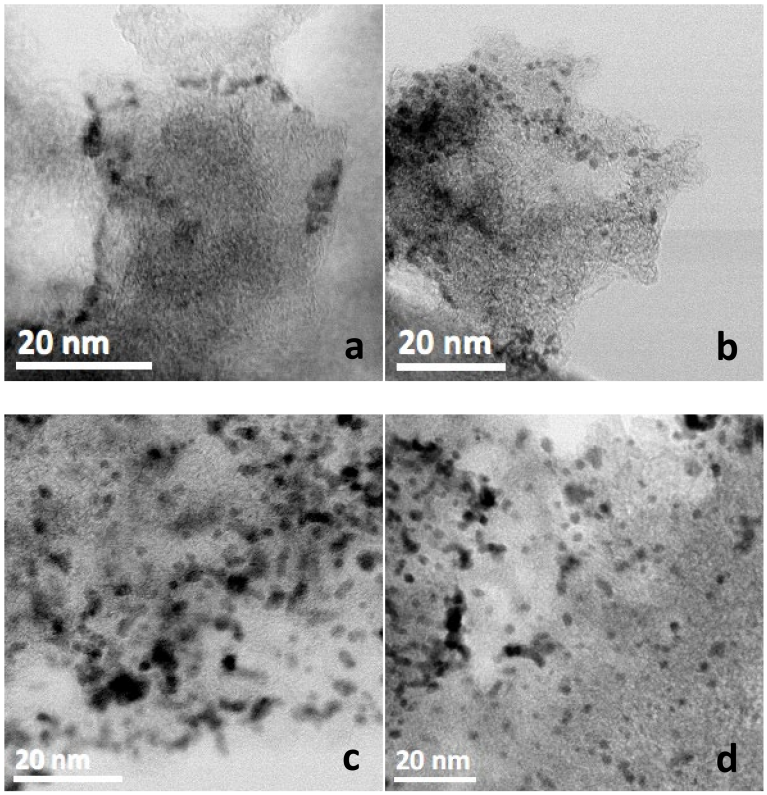

Figure 4. HR-TEM images for (**a**) RuO_2 (5%)/AC; (**b**) RuO_2 (5%)–pre-treated SO_3H/AC; (**c**) RuO_2 (5%)/AC after 5 runs; (**d**) RuO_2 (5%)–pre-treated SO_3H/AC after 5 runs.

2.2. Cellulose Transformation into Sorbitol

Due to its insolubility in water, cellulose has difficulties reacting in this medium. This is why a variety of pre-treatments can be conducted to make cellulose more reactive, as explained in the Introduction [42–45]. In our case, a ball-milling step for 24 h prior to catalysis was chosen. The conditions are detailed in the Experimental Section. First, the reactivity of our bifunctional catalyst with and without prior ball milling of the cellulose was assessed (Table 9).

Table 9. Hydrogenolysis of cellulose with bifunctional catalyst (RuO_2 (5%)–pre-treated SO_3H/AC). cellulose conversion; xylitol, mannitol and sorbitol selectivities; sorbitol yield (150 °C, 30 bar of H_2, 2 h, 150 mg of catalyst, 1 g of cellulose). The estimated confidence interval for cellulose conversion and selectivities is 5%.

Pre-Treatment	Cellulose Conversion (%)	Xylitol Selectivity (%)	Mannitol Selectivity (%)	Sorbitol Selectivity (%)	Sorbitol Yield (%)
No ball milling	20	7	0	10	2
Ball milling (300 rpm)	25	11	7	28	7

Cellulose conversion is calculated, as described in the Experimental Section. As this is calculated by weighing the cellulose after the catalytic reaction, the conversion of cellulose presented in the article is the lowest possible conversion (underestimation) because all the recovered mass is attributed to cellulose, but it could potentially be side products that are also solid, such as humins. Cellulose conversion under these soft conditions (150 °C) is low. The ball milling of cellulose enhanced its reactivity, and increases in both sorbitol conversion and selectivity was obtained compared to without milling. Two side products were identified, namely, xylitol and mannitol. Mannitol comes from the isomerization of sorbitol, while xylitol is produced by the decarbonylation of sorbitol [46]. These side products were not present in the catalytic tests on cellobiose. The mechanism of hydrolysis and hydrogenation must be slightly different when starting from a soluble glucose dimer (cellobiose) than from an insoluble polymer (cellulose), which explains the difference in side-product formation. Perhaps small oligomers with more than two units are formed from cellulose, which can go through other reaction routes. Traces (<1%) of cellobiose and glucose can also be seen on the chromatograms, but this was not indicated in the results table for the sake of clarity and readability.

The temperature was varied to see its impact on the reaction. In order to improve cellulose reactivity, the temperature was increased to 170 °C and 190 °C (Table 10). The impact of temperature on cellulose conversion is striking: a slight increase at 170 °C and a huge improvement at 190 °C were observed. However, the sorbitol selectivity stayed around 30%, with a maximum of 34% at 170 °C. Indeed, it is known that increasing the temperature will favor sorbitol degradation [42]. A test at 190 °C for 24 h was conducted and confirmed that sorbitol selectivity drops when high temperatures and long reaction times are applied. However, the cellulose conversion reached almost 100%, and the global yield of sorbitol (20%) was the same for both conditions. The optimal conditions to maximize the sorbitol yield should be somewhere between 2 h and 24 h. Unfortunately, kinetic studies are difficult to build on this reaction. Indeed, as cellulose is not soluble in water, the solid has to be weighed after filtration to calculate the cellulose conversion by subtracting the catalyst mass from the final combined mass. Aliquots cannot be taken during the reaction to have enough data points in order to build a full kinetic curve.

Table 10. Hydrogenolysis of cellulose with bifunctional catalyst (RuO_2 (5%)–pre-treated SO_3H/AC). Cellulose conversion; xylitol, mannitol and sorbitol selectivities; sorbitol yield (30 bar of H_2, 150 mg of catalyst, 1 g of ball-milled cellulose (300 rpm)). The estimated confidence interval for cellulose conversion and selectivities is 5%.

Temperature and Time	Cellulose Conversion (%)	Xylitol Selectivity (%)	Mannitol Selectivity (%)	Sorbitol Selectivity (%)	Sorbitol Yield (%)
150 °C/2 h	25	11	7	28	7
170 °C/2 h	35	8	6	34	12
190 °C/2 h	70	3	5	30	21
190 °C/24 h	98	2	4	20	20

A comparison between the monofunctional and the bifunctional catalysts was conducted with two different reaction conditions: at 150 °C for 24 h and at 190 °C for 2 h (Table 11). The results indicate that the same cellulose conversion was obtained with both catalysts. However, the bifunctional catalyst produced almost twice the amount of sorbitol. Side products, such as xylitol and mannitol, formed less with the bifunctional catalyst. The same effect of sorbitol stabilization, as was shown in the previous section, can be observed here. This highlights the synergy between the Ru and sulfonic functions and confirms that the bifunctional catalyst is definitely better than the monofunctional catalyst for sorbitol production.

Table 11. Hydrogenolysis of cellulose with monofunctional and bifunctional catalysts. Cellulose conversion; xylitol, mannitol and sorbitol selectivities; sorbitol yield (30 bar of H_2, 150 mg of catalyst, 1 g of ball-milled cellulose (300 rpm)). The estimated confidence interval for cellulose conversion and selectivities is 5%.

Catalyst	Cellulose Conversion (%)	Xylitol Selectivity (%)	Mannitol Selectivity (%)	Sorbitol Selectivity (%)	Sorbitol Yield (%)
RuO_2 (5%)/AC [a]	43	7	12	21	9
RuO_2 (5%)–pre-treated SO_3H/AC [a]	44	6	5	37	16
RuO_2 (5%)/AC [b]	69	8	15	13	9
RuO_2 (5%)–pre-treated SO_3H/AC [b]	70	3	5	30	21

[a] 150 °C for 24 h; [b] 190 °C for 2 h.

In order to maximize the sorbitol yield, a new pre-treatment was set up. As cellulose is not soluble in water, increasing its proximity to the catalyst should enhance its reactivity. This is why combined ball-milling pre-treatment of the cellulose with the catalyst was implemented just before starting the reaction. This ball milling is shorter than the pre-treatment of cellulose alone, only 2 h, and is detailed in the Experimental Section. Cellulose is still ball-milled for 24 h before the second pre-treatment. The results obtained by doing so are presented in Table 12. If these results are compared with the results without the ball milling of both cellulose and catalyst together (Table 10), it can be seen that combined ball milling has a positive impact on the results. Cellulose conversion increased for all temperatures. The sorbitol selectivity remained the same for the test at 150 °C, but it increased drastically for the tests at 170 °C and 190 °C. With this new method, almost 40% of sorbitol yield can be reached at 190 °C in only 2 h directly from cellulose. A catalytic test with the monofunctional catalyst was conducted similarly, and the results were also better when implementing combined ball milling. However, it was confirmed that the bifunctional catalyst is far better than the monofunctional one even under the new conditions.

Table 12. Hydrogenolysis of cellulose with monofunctional and bifunctional catalysts. Cellulose conversion; xylitol, mannitol and sorbitol selectivities; sorbitol yield (30 bar of H_2, 2 h, 150 mg of catalyst, 1 g of ball-milled cellulose (300 rpm) with combined ball milling). The estimated confidence interval for cellulose conversion and selectivities is 5%.

Conditions	Cellulose Conversion (%)	Xylitol Selectivity (%)	Mannitol Selectivity (%)	Sorbitol Selectivity (%)	Sorbitol Yield (%)
150 °C plus bifunctional catalyst	33	6	6	28	9
170 °C plus monofunctional catalyst	40	8	13	33	13
170 °C plus bifunctional catalyst	52	5	6	50	26
190 °C plus bifunctional catalyst	73	2	6	54	39

As the combined ball milling of the cellulose and the catalyst extended the total ball-milling time of cellulose by 2 h, it is reasonable to question if this increase in activity is due to the extra ball-milling duration or primarily due to the proximity between the cellulose and the catalyst. A catalytic test with cellulose pre-treated for 26 h was carried out to address this issue (Table 13). The results show that the ball milling of cellulose for 26 h slightly increased the activity compared to 24 h ball milling. However, the combined ball milling of both cellulose and the catalyst still provided the best results. It can be

concluded that combined ball milling has a real effect on the reactivity between cellulose and the catalyst.

Table 13. Hydrogenolysis of cellulose with bifunctional catalyst (RuO_2 (5%)–pre-treated SO_3H/AC). Cellulose conversion; xylitol, mannitol and sorbitol selectivities; sorbitol yield (170 °C, 30 bar of H_2, 2 h, 150 mg of catalyst, 1 g of ball-milled cellulose (300 rpm) with and without combined ball milling). The estimated confidence interval for cellulose conversion and selectivities is 5%.

Conditions	Cellulose Conversion (%)	Xylitol Selectivity (%)	Mannitol Selectivity (%)	Sorbitol Selectivity (%)	Sorbitol Yield (%)
170 °C plus combined ball milling	52	5	6	50	26
170 °C with 26 h ball-milled cellulose (no combined ball milling)	37	5	7	38	14

2.3. Benchmarking

As the superiority of bifunctional catalysts over the monofunctional catalyst has now been demonstrated, it is time to compare our results with the literature. In order to do that, two catalytic tests were carried out using another cellulose grade: Avicel PH-101 (Table 14). Indeed, this grade was selected as it is the most common type that can be found in the literature in similar studies [45]. Surprisingly, the results here are almost the same without and with the combined ball milling of both catalyst and cellulose before the reaction. Only a slight increase in cellulose conversion can be observed when implementing combined ball milling. If these results are compared with the ones obtained with the other cellulose type, as described above, it can be noticed that the Avicel PH101 cellulose produces a little less sorbitol under the same conditions. As these results are almost similar to the ones obtained with the first cellulose grade, all the conclusions that are established above can obviously stand for this second cellulose type.

Table 14. Hydrogenolysis of cellulose with bifunctional catalyst (RuO_2 (5%)–pre-treated SO_3H/AC). Cellulose conversion; xylitol, mannitol and sorbitol selectivities; sorbitol yield (190 °C, 30 bar of H_2, 2 h, 150 mg of catalyst, 1 g of ball-milled cellulose (300 rpm) with and without combined ball milling). The estimated confidence interval for cellulose conversion and selectivities is 5%.

Catalyst	Cellulose Conversion (%)	Xylitol Selectivity (%)	Mannitol Selectivity (%)	Sorbitol Selectivity (%)	Sorbitol Yield (%)
RuO_2 (5%)–pre-treated SO_3H/AC without combined ball milling	64	0	4	38	24
RuO_2 (5%)–pre-treated SO_3H/AC with combined ball milling	71	0	4	38	27

The results obtained under the best possible conditions, using the Avicel PH-101 cellulose, allow us to compare our results with the literature and to benchmark the performance obtained in comparison to all the other catalysts envisaged for sorbitol production. It should be noted that comparisons must be performed based on sorbitol yields, which are quantified in the catalytic test filtrates, rather than relying on solid residues, which may also contain humins.

Table 15 lists the sorbitol production obtained directly from cellulose with various Ru-based catalysts. A comparison between the literature results and our work is not an easy task because of the differences in the reaction conditions. By looking at entry 1, it can be observed that sorbitol was produced from crystalline cellulose with a monofunctional

Ru catalyst in a short reaction time but at a very high reaction temperature (245 °C versus 190 °C in the present study). The best catalyst presented in this work shows a similar result at lower temperatures with joint ball milling and longer reaction times (entry 13). Entry 2 showed similar sorbitol productivity and used the same reaction conditions as our work, except for the reaction time and Ru loading. This highlights the improvement in catalyst activity by the sulfonic functions and the ball-milling procedure. Entries 3 and 4 used bifunctional catalysts with Ru nanoparticles on AC doped with heteropolyacids. Despite the harsh reaction conditions (lower cellulose/catalyst ratios, longer reaction times and higher temperatures), the sorbitol yields obtained by these authors were lower than the ones obtained with the catalysts that were made in this work. The fact that the joint ball-milling step slightly decreased the sorbitol yield, in their case, is unexpected. Similar bifunctional catalysts using Ru and SO_3H-AC (sulfonation was achieved by using concentrated H_2SO_4) were used (entries 5 and 6) with 10 wt.% of Ru loading. The difference without and with joint ball milling is striking, and this shows that joint ball milling can lead to excellent sorbitol production. Higher Ru loading, lower substrate/catalyst ratios and longer reaction times can explain the better activity of this catalyst compared to ours despite the lower reaction temperature. Entries 7 and 8 used the same type of catalyst as us with the same Ru loading. However, in their case, 5 wt.% of Ru led to lower selectivity in hexitols (the authors did not separate the sorbitol and mannitol selectivities). Despite using lower substrate/catalyst ratios and longer reaction times, the results they obtained are quite similar to ours, which indicates that our catalyst again seems to be more active. Nevertheless, such comparisons are very delicate because the impact of each variation in experimental conditions is difficult to predict. Sulfonated silica with Ru can be used to produce sorbitol at low temperatures with low cellulose/catalyst ratios and longer reaction times (entry 9). Entry 10 provided the results for a bifunctional catalyst with Ru on an acidic zeolite. A low yield of sorbitol was obtained, but this can be attributed to the use of microcrystalline cellulose as a substrate. The last two entries (11 and 12) used a mix of two catalysts—Ru on mesoporous carbon and an acidic catalyst (ZrP). Once again, the joint ball milling of cellulose with the catalysts drastically improved the sorbitol yield. Globally, our best catalyst is very efficient, and the sorbitol yield we obtained is competitive with the literature results. Moreover, our reaction conditions with high cellulose/catalyst ratios and short reaction times are beneficial for possible industrial applications.

Table 15. Transformation of cellulose into sorbitol from the literature.

Entry	Catalyst	Cellulose Pre-Treatment	Cellulose/ Catalyst Mass (mg)	Substrate Concentration (mg/mL)	Time (h)	Temperature (°C)	Cellulose Conversion (%)	Sorbitol Yield (%)	Mannitol Yield (%)	Sorbitol Productivity (mmol g^{-1} of Catalyst h^{-1})	Ref.
1	4 wt.% Ru/AC	Microcrystalline cellulose	1000/100	20.0	0.5	245	86	30	10	33.30	[47]
2	2 wt.% Ru/AC	Ball milling	324/50	10.8	18	190	83	30	8	0.60	[48]
3	0.4 wt.% Ru/AC–TPA ($H_3O_{40}PW_{12}{\cdot}nH_2O$)	Ball milling	750/300	2.5	6	205	98	16	n.d.	0.37	[49]
4	0.4 wt.% Ru/AC–TPA ($H_3O_{40}PW_{12}{\cdot}nH_2O$)	Joined ball milling	750/300	2.5	6	205	100	13	n.d.	0.30	[49]
5	10 wt.% Ru/AC-SO_3H	Microcrystalline cellulose	50/20	4.2	24	165	20	9	4	0.05	[50]
6	10 wt.% Ru/AC-SO_3H	Ball milling	50/20	4.2	24	165	81	59	7	0.34	[50]
7	3 wt.% Ru/AC-SO_3H	Ball milling	1120/480	28.0	24	180	95	Sum = 42		N/A	[51]
8	5 wt.% Ru/AC-SO_3H	Ball milling	1120/480	28.0	24	180	95	Sum = 10		N/A	[51]
9	3 wt.% Ru/SiO_2-SO_3H	Ball milling	250/200	33.3	10	150	90	61	7	0.42	[31]
10	3 wt.% Ru/BEA zeolite	Microcrystalline cellulose	140/60	28.0	24	180	35	21	n.d.	0.11	[52]
11	ZrP (900 mg)—3 wt.% Ru/MC (mesoporous carbon)	Microcrystalline cellulose	500/30	10.0	1.5	170	34	21	1	12.95	[53]
12	ZrP (900 mg)—3 wt.% Ru/MC	Joined ball milling	500/30	10.0	1.5	170	100	66	2	40.71	[53]
13	RuO_2 (5%)—pre-treated SO_3H/AC	Joined ball milling	1000/150	8.3	2	190	71	27	3	5.00	Our work

n.d. = non determined.

3. Experimental Section

3.1. Reagents and Materials

The activated carbon (AC; SX+ type) (Boehm acidity: 42 mmol/100 g) was obtained from NORIT (Amersfoort, The Netherlands). Sulfanilic acid (99%), isopentyl nitrite (96%), ruthenium (III) chloride hydrate, hydrogen peroxide (H_2O_2) (30% *w*/*w* in water), glucose, mannitol, xylitol, sorbitol, D-(+)-cellobiose (≥99%), cellulose (reference C6288, crystalline and high purity) were supplied by Sigma-Aldrich Belgium branch (Darmstadt, Germany) and used as received.

3.2. Catalysts Preparation

3.2.1. Acidic Functionalization

The carbon functionalization was carried out by a diazonium coupling method (Scheme 2) [54]. Typically, 1 g of carbon powder was dispersed in 60 mL of distilled water. A total of 1.5 g of sulfanilic acid was added, and the suspension was stirred at 70 °C for 10 min. The suspension was cooled down to 30 °C before adding 1.2 mL of isopentyl nitrite. The mixture was stirred for 16 h. Then, it was filtered out and washed with distilled water and ethanol. The resulting material was dried overnight at 100 °C.

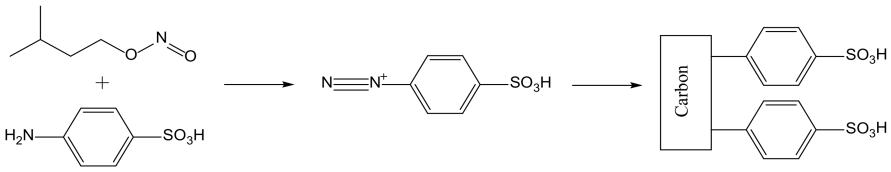

Scheme 2. Diazonium coupling on carbon materials for sulfonic acid grafting.

3.2.2. Heat Treatment

Catalysts were thermally treated at different temperatures to modulate the amount of surface sulfonic functions. In order to do this, solids were placed in a tubular oven and heated under N_2 to 200 °C, 300 °C or 400 °C with an increase in temperature of 100 °C/h. When the targeted temperature was reached, it was maintained for 2 h before being decreased to room temperature naturally.

3.2.3. Ru Nanoparticles Deposition

A colloidal suspension of RuO_2 was synthesized via slow hydrolysis/condensation of $RuCl_3$ by using H_2O_2 as oxidizing agent. It was adapted from a literature procedure [41]. In order to have 1 wt.% of Ru on the carbon support, 24.8 mg of $RuCl_3$ was added to 40 mL of demineralized water (solution A), and 1 mL of H_2O_2 (35% in volume) was added to 20 mL of demineralized water (solution B). Solution B was added drop-by-drop to solution A. The final mixture was agitated for 5 min. After this, a Berlin glass flask capped with aluminum foil containing the mixture was placed in an oven at 95 °C for 2 h. The solution was cooled down to room temperature and added to 1 g of AC. The dispersion was agitated for 30 min. The solid was recovered by evaporation of the solvent in a rotavapor at 60 °C under reduced pressure, and it was dried overnight at 100 °C.

For synthesizing the bifunctional catalysts with 3 wt.% and 5 wt.% of Ru, the amount of $RuCl_3$ engaged in the syntheses was adapted to fit the targeted percentages, with all other variables kept constant.

3.2.4. Cellulose Pre-Treatment

Ball milling was performed with a Fritsch Pulverisette 7 premium line apparatus. All experiments were carried out in stainless-steel milling bowls of 45 mL (Fristch™ 50.9750.00). A total of 10 g of cellulose and five stainless-steel balls of 10 mm (Fritsch™ 55.0100.09) were used for each pre-treatment. Millings were carried out at room temperature (20 °C), the local heating during milling was not monitored in situ, but milling pauses (breaks) were

introduced to limit potential overheating. The complete cycle was composed of 15 min of ball milling at 300 rpm followed by 5 min of pause. A total of 96 cycles were performed for a total ball-milling time of 24 h.

Combined ball milling with both catalyst and cellulose was carried out with the same device but with different conditions: 1 g of cellulose and 150 mg of catalyst were placed together with three stainless-steel balls. This treatment was performed for 8 cycles at 300 rpm (total of 2 h).

3.3. Catalytic Tests

The tests were carried out in a 250 mL stainless-steel Parr autoclave. A total of 1 g of cellobiose or cellulose was added to 150 mg of catalyst in 120 mL of mQ water. This low substrate concentration ensures absence of diffusional limitations. Then, the autoclave was sealed, and the system was purged three times with nitrogen and heated up under autogenic pressure of N_2 for the hydrolysis tests and under 30 bar of H_2 for the hydrogenation tests (this pressure was set when the temperature was reached). For the controlled temperature, the agitation was started at 1700 rpm. After the fixed duration of catalytic test, the system was then cooled down to room temperature, and the solution was filtrated. The solid catalyst was washed with mQ water and dried. The filtrate was then diluted to 250 mL with mQ water in order to always have the same final volume so that all results could be strictly comparable and analyzed by using HPLC. For kinetic studies, at various time intervals, liquid aliquots (~1–2 mL) were taken and diluted two times with mQ water before analyzing it similarly. The pressure within the autoclave was brought back to 30 bar of H_2 after each sampling.

Consecutive reactions were performed as follows: First, hydrogenation using the RuO_2/AC catalyst was carried out, as described above, under 30 bar of H_2, and then, the solid was filtered out. Consecutively, the SO_3H/AC catalyst was added to the filtrate, and the hydrolysis test was performed, as described above under N_2.

The opposite consecutive reactions were performed with the same methodology by doing first the hydrolysis reaction using the SO_3H/AC catalyst under N_2. Then, the solid was filtered out and RuO_2/AC catalyst was added to the filtrate. Finally, the hydrogenation was performed under 30 bar of H_2.

Recyclability tests were performed by re-using catalysts obtained by filtration after a catalytic test. The recovered solid was first washed with mQ water and dried overnight at 100 °C in air. If the catalyst mass was below 150 mg, fresh catalyst that had not been used before was added to maintain the same catalyst quantity for each test. The added mass was never more than 10% of the total.

HPLC analyses were performed with a Waters system equipped with Waters 2414 refractive index (RI) detector (detector temperature, 30 °C). The column used for the analyses is an Aminex HPX 87C column, with mQ H_2O (18 MΩ.cm at 25 °C) as eluent, a flux of 0.5 mL/min, a column temperature of 85 °C and 25 µL of injected volume. For cellobitol quantification, a calibration curve for cellobiose was used, with the assumption that they have similar refractive indexes.

The conversion of cellobiose is calculated as follows:

$$\text{Cellobiose conversion } (\%) = \frac{\text{n cellobiose converted}}{\text{initial n cellobiose}} \times 100$$

The glucose selectivity is calculated as follows:

$$\text{Glucose selectivity } (\%) = \frac{\text{n glucose produced}}{2 \times (\text{n cellobiose converted})} \times 100$$

The sorbitol selectivity is calculated as follows:

$$\text{Sorbitol selectivity } (\%) = \frac{\text{n sorbitol produced}}{2 \times (\text{n cellobiose converted})} \times 100$$

The cellobitol selectivity is calculated as follows:

$$\text{Cellobitol selectivity } (\%) = \frac{\text{n cellobitol produced}}{\text{n cellobiose converted}} \times 100$$

The glucose yield from cellobiose is calculated as follows:

$$\text{Glucose yield } (\%) = \frac{\text{n glucose produced}}{2 \times \text{initial n cellobiose}} \times 100$$

The sorbitol yield from cellobiose is calculated as follows:

$$\text{Sorbitol yield } (\%) = \frac{\text{n sorbitol produced}}{2 \times \text{initial n cellobiose}} \times 100$$

For the catalytic reaction on cellulose substrate, the formulae are slightly different. The conversion of cellulose is calculated as follows:

$$\text{Cellulose conversion } (\%) = \frac{(\text{initial cellulose mass} - \text{recovered cellulose mass})}{\text{initial cellulose mass}} \times 100$$

$$\text{Recovered cellulose mass} = \text{ Total mass after filtration} - \text{initial catalyst mass}$$

The glucose selectivity is calculated as follows:

$$\text{Glucose selectivity } (\%) = \frac{\text{n glucose produced}}{(\text{n glucose unit converted})} \times 100$$

The sorbitol selectivity is calculated as follows:

$$\text{Sorbitol selectivity } (\%) = \frac{\text{n sorbitol produced}}{(\text{n glucose unit converted})} \times 100$$

The xylitol selectivity is calculated as follows:

$$\text{Xylitol selectivity } (\%) = \frac{\text{n xylitol produced}}{(\text{n glucose unit converted})} \times 100$$

The mannitol selectivity is calculated as follows:

$$\text{Mannitol selectivity } (\%) = \frac{\text{n mannitol produced}}{(\text{n glucose unit converted})} \times 100$$

The glucose yield from cellulose is calculated as follows:

$$\text{Glucose yield } (\%) = \frac{\text{n glucose produced}}{\text{initial n glucose unit}} \times 100$$

The sorbitol yield from cellulose is calculated as follows:

$$\text{Sorbitol yield } (\%) = \frac{\text{n sorbitol produced}}{\text{initial n glucose unit}} \times 100$$

For all the formulae above, the n glucose unit is calculated as follows:

$$\text{n anhydroglucose unit} = \frac{\text{cellulose mass}}{\text{molar mass of anhydroglucose unit}}$$

3.4. Characterization Methods

XPS analyses were carried out at room temperature with an SSI-Xprobe (SSX 100/206) photoelectron spectrometer from Surface Science Instruments (SSI, Moutain View, CA, USA), equipped with a monochromatized microfocus Al X-ray source. Samples were stuck onto small sample holders with double-sided adhesive tape and then placed on an insulating ceramic carousel (Macor®, Moutier, Switzerland). Charge effects were avoided by placing a nickel grid above the samples and using a flood gun set at 8 eV. The binding energies were calculated with respect to the C-(C, H) component of the C_{1s} peak fixed at 284.4 eV. Data treatment was performed using the CasaXPS program (Casa Software Ltd., Teignmouth, Devon, UK). The peaks were decomposed into a sum of Gaussian/Lorentzian (85/15) after subtraction of a Shirley-type baseline. Only Ru_{3d} peaks were used to determine Ru at. % and its oxidation state in all catalysts.

Powder X-ray diffraction (PXRD) patterns were recorded at room temperature on a Siemens D5000 diffractometer equipped with a Ni filter using CuKα radiation (Bragg-Brentano geometry) operated at 40 kV and 40 mA. Diffractograms were taken between 5° and 80° (2θ) with a step size of 0.02° (2θ).

Boehm titration method was used to evaluate catalyst acidity [55,56]. NaOH solutions were prepared via dilution of Titrisol ampoules (VWR) containing precise and known quantities of sodium hydroxide. HCl solutions were prepared via the dilution of concentrated hydrochloric acid. The HCl concentrations were determined by titration with the standard NaOH solutions. These solutions were prepared with mQ water that was previously decarbonated by nitrogen flushing. For titrating the acid groups, 60 mg of sample was dispersed in 30 mL of NaOH 0.01 mol/L, and the solution was decarbonized for 1 h under Ar flux. The mixture was then agitated for 23 h under Ar atmosphere. The suspension was then filtrated and 10 mL of the resulting filtrate was back-titrated (repeated twice) under Ar flux using a HCl 0.005 mol/L solution. The indicator used was phenolphthalein. The amount of acid functions on the catalyst was determined by calculating the difference between the initial amount of NaOH and the amount of NaOH titrated by the HCl.

HR-TEM analyses were carried out on a JEOL 2100 FEG S/TEM working at 200 kV voltage, equipped with a probe corrector for spherical aberrations. For these measurements, samples were dispersed in an ethanol solution and a drop of each suspension was deposited on a copper grid covered with a holey carbon membrane.

STEM analyses were carried out on a JEOL 2100 FEG S/TEM by using a spot size of 0.13 nm with a current density of 140 pA and a camera focal distance of 8 cm, corresponding to inside and outside annular detector diameters of 73 and 194 mrad. EDX mapping was performed using a JEOL Silicon Drift Detector (SDD) with sensor size of 60 mm^2.

Total organic content (TOC) analyses were performed on solutions after catalytic tests by using a Shimadzu TOC-L analyzer with an ASI-L autosampler using the combustion catalytic oxidation method at 680 °C.

4. Conclusions

Bifunctional catalysts with sulfonic functions and RuO_2 nanoparticles were synthesized with the aim of directly transforming cellulose into sorbitol (two-step reaction of combined hydrolysis/hydrogenation). The sulfonic function amount was controlled by heat treatment at different temperatures and with pre-treatment under the same conditions as the catalytic test. These modifications allowed us to obtain different ratios between the sulfonic functions and the Ru amounts. It was shown that high amounts of sulfonic functions completely inhibit Ru active sites, and in this case, mainly glucose (a hydrolysis product) was obtained at the end of the reaction, starting from cellobiose as the model molecule. With a higher amount of Ru (5 wt.%), a very efficient bifunctional catalyst was obtained, and its activity outmatched the monofunctional catalyst. The kinetic studies on the monofunctional and bifunctional catalysts showed a striking difference between the two systems. Indeed, with the monofunctional catalyst, sorbitol degraded during the reaction, and the sorbitol yield after 24 h was very low, while the bifunctional catalyst played

a stabilizing role for sorbitol and provided a very high yield of it. This was confirmed via a degradation test of sorbitol with both catalysts. The synergy between the sulfonic functions and the Ru nanoparticles was demonstrated by these results. Sulfonic functions stabilize the sorbitol and, therefore, increase the yield; however, it is a subtle balance, as too many sulfonic functions can poison Ru. The recyclability tests showed that the bifunctional catalyst was more stable than the monofunctional one, even if both catalysts suffered from slight deactivation during the first run. Catalyst stability was confirmed with TEM and EDX analyses before and after the reaction. Ru nanoparticle size only slightly increased after five consecutive reactions, and sulfur remained evenly distributed over the entirety of the support.

Finally, the best bifunctional catalyst was assessed for the direct transformation of cellulose into sorbitol. Sorbitol was successfully obtained from cellulose, and the bifunctional catalyst clearly provided better activity than the monofunctional one. The importance of cellulose pre-treatment was demonstrated with the better results obtained when ball milling was applied. Moreover, the combined ball milling of cellulose with the catalyst before the reaction showed outstanding results, as it doubled sorbitol yield (from 21% to 39% within 2 h). The transformation of another crystalline cellulose (Avicel PH101) was carried out with the bifunctional catalyst in order to more easily compare our results with the existing literature. Comparisons with other active metals for this transformation are important, and using a low amount of Ru to achieve a high sorbitol yield could be more interesting than using high quantities of Ni for the same price, especially given that Ru is more resistant to oxidation and leaching than Ni. Moreover, more active metals are more suitable for complex substrates, such as raw cellulose. This comparison with the literature shows that our bifunctional catalyst is efficient and can compete with other systems for sorbitol production.

Supplementary Materials: The following supporting information can be downloaded at: https://www.mdpi.com/article/10.3390/catal13060963/s1, S1. S_{2p} peaks from XPS analyses for the SO_3H/AC catalyst without heat-treatment and with heat-treatment at 200 °C, 300 °C and 400 °C; Figure 1: S_{2p} peak from XPS analysis for SO_3H/AC catalyst without heat-treatment; Figure 2: S_{2p} peak from XPS analysis for SO_3H/AC catalyst heat-treated at 200 °C; Figure 3: S_{2p} peak from XPS analysis for SO_3H/AC catalyst heat-treated at 300 °C; Figure 4: S_{2p} peak from XPS analysis for SO_3H/AC catalyst heat-treated at 400 °C; S2. Kinetic curves for bifunctional catalysts prepared with different SO_3H heat- treatments; Figure 5: Kinetic curves for the transformation of cellobiose into sorbitol with RuO_2 (1 wt.%)–SO_3H treated at 200 °C/SX+ catalyst; the lines connecting experimental points are only a visual aid and do not correspond to any mathematical model; Figure 6: Kinetic curves for the transformation of cellobiose into sorbitol with RuO_2 (1 wt.%)–SO_3H treated at 300 °C/SX+ catalyst; the lines connecting experimental points are only a visual aid and do not correspond to any mathematical model; Figure 7: Kinetic curves for the transformation of cellobiose into sorbitol RuO_2 (1 wt.%)–SO_3H treated at 400 °C/SX+ catalyst; the lines connecting experimental points are only a visual aid and do not correspond to any mathematical model; S3. S_{2p} peaks and atomic percentages from XPS analyses for the pre-treated SO_3H/AC catalyst; Figure 8: S_{2p} peak from XPS analyses of pre-treated SO_3H/SX+; Table 1: Oxygen and sulfur contents determined by XPS of the acidic catalysts without pre-treatment and with pre-treatment in the same condition as catalytic tests; S4. Conversion of cellobiose, selectivity and yield in sorbitol corresponding to the kinetic curves in main text in Figure 1; Table 2: Results of the kinetic study for the hydrogenolysis of cellobiose with RuO_2 (5 wt.%)/AC; Cellobiose conversion, selectivity in glucose, cellobitol and sorbitol, yield in sorbitol (150 °C, 30 bar of H_2, 24 h, 150 mg of catalyst); Table 3: Results of the kinetic study for the hydrogenolysis of cellobiose with RuO_2 (5 wt.%)–pre-treated SO_3H/AC; Cellobiose conversion, selectivity in glucose, cellobitol and sorbitol, yield in sorbitol (150 °C, 30 bar of H_2, 24 h, 150 mg of catalyst); S5. List of molecules injected in HPLC; Table 4: List of molecules analyzed by HPLC and observation of their presence or not in catalytic tests; S6. C_{1s} and Ru_{3d} peaks from XPS analyses for different AC supported catalysts; Figure 9: C_{1s} and Ru3d peaks from XPS analyses of RuO_2 (5 wt. %)/AC catalyst; Figure 10: C1s and Ru_{3d} peaks from XPS analyses of RuO_2 (5 wt. %)–pre-treated SO_3H/AC catalyst; Figure 11: C_{1s} and Ru_{3d} peaks from XPS analyses of RuO_2 (5 wt. %)/AC catalyst after 5 runs; Figure 12: C1s and Ru_{3d} peaks from XPS analyses of RuO_2 (5 wt. %)–pre-treated SO_3H/AC catalyst after 5 runs;

S7. Atomic percentage of C_{1s} and Ru_{3d} from XPS analyses of monofunctional and bifunctional catalysts with 3 wt.% of Ru; Table 5: Atomic ratio of C_{1s} and Ru_{3d} for RuO_2 (3 wt.%)/AC and RuO_2 (3 wt.%)–pre-treated SO_3H/AC; S8. HR-TEM, STEM and EDX mapping analyses for monofunctional and bifunctional catalysts, before and after catalytic reaction; Figure 13: HR-TEM, STEM and EDX mapping analyses for RuO_2 (5%)/AC before catalytic test; Figure 14: HR-TEM, STEM and EDX mapping analyses for RuO_2 (5%)–pre-treated SO_3H/AC before catalytic test; Figure 15: HR-TEM, STEM and EDX mapping analyses for RuO_2 (5%)/AC after 5 runs; Figure 16: HR-TEM, STEM and EDX mapping analyses for RuO_2 (5%)–pre-treated SO_3H/AC after 5 runs; S9. Comparison of Ru regions from XPS analyses before and after several catalytic runs; Figure 17: XPS ruthenium regions for: (TOP) RuO_2 (5%)/AC; (BOTTOM) RuO_2 (5%)–pre-treated SO_3H/AC; Figure 18: XPS ruthenium regions for: (TOP) RuO_2 (5%)/AC after 4 runs; (BOTTOM) RuO_2 (5%)–pre-treated SO_3H/AC after 5 runs; Figure 19: XPS Ru 3p regions for: (LEFT) RuO_2 (5%)/AC before (black) and after 4 runs (blue); (RIGHT) RuO_2 (5%)–pre-treated SO_3H/AC before (black) and after 5 runs (blue).

Author Contributions: S.C.: Investigation, Formal analysis, Methodology, Visualization, Writing—original draft; W.B.: Investigation, Visualization, Writing—review & editing; O.E.: Validation, Writing—review & editing; S.H.: Conceptualization, Funding acquisition, Methodology, Project administration, Supervision, Validation, Writing—review & editing. All authors have read and agreed to the published version of the manuscript.

Funding: This research was funded by Université catholique de Louvain though a teaching assistant post for Samuel Carlier and by F.R.S.—FNRS through a Research Director post for Sophie Hermans. It received no other external funding.

Data Availability Statement: The data presented in this study is available within the article or Supplementary Material.

Acknowledgments: The authors wish to thank the Fonds de la Recherche Scientifique (F.R.S.—FNRS) and the Université catholique de Louvain (Belgium) for funding. We are grateful to Jean François Statsyns for lab technical assistance, Pierre Eloy for XPS analyses and useful discussions, François Devred for XRD analyses and Laurent Collard for HPLC technical assistance.

Conflicts of Interest: The authors declare no conflict of interest.

References

1. Deng, W.; Feng, Y.; Fu, J.; Guo, H.; Guo, Y.; Han, B.; Jiang, Z.; Kong, L.; Li, C.; Liu, H.; et al. Catalytic conversion of lignocellulosic biomass into chemicals and fuels. *Green Energy Environ.* **2023**, *8*, 10–114. [CrossRef]
2. Jha, S.; Okolie, J.A.; Nanda, S.; Dalai, A.K. A Review of Biomass Resources and Thermochemical Conversion Technologies. *Chem. Eng. Technol.* **2022**, *45*, 791–799. [CrossRef]
3. Parajuli, R.; Dalgaard, T.; Jørgensen, U.; Adamsen, A.P.S.; Knudsen, M.T.; Birkved, M.; Gylling, M.; Schjørring, J.K. Biorefining in the prevailing energy and materials crisis: A review of sustainable pathways for biorefinery value chains and sustainability assessment methodologies. *Renew. Sustain. Energy Rev.* **2015**, *43*, 244–263. [CrossRef]
4. Li, H.; Fang, Z.; Smith, R.L.; Yang, S. Efficient valorization of biomass to biofuels with bifunctional solid catalytic materials. *Prog. Energy Combust. Sci.* **2016**, *55*, 98–194. [CrossRef]
5. Sarra, M.; Rouissi, T.; Brar, S.K.; Blais, J.F. Chapter 4—Life Cycle Analysis of Potential Substrates of Sustainable Biorefinery. In *Platform Chemical Biorefinery*; Elsevier: Amsterdam, The Netherlands, 2016; pp. 55–76. [CrossRef]
6. Menon, V.; Rao, M.; Prakash, G. Value added products from hemicellulose—Biotechnological perspective. *Glob. J. Biochem.* **2010**, *1*, 36–67. Available online: https://www.semanticscholar.org/paper/Value-added-products-from-hemicellulose%3A-Menon-Prakash/ae5ae4e306d715a35734623965fa73ee97a51b16 (accessed on 30 March 2023).
7. Ruppert, A.M.; Weinberg, K.; Palkovits, R. Hydrogenolysis goes bio: From carbohydrates and sugar alcohols to platform chemicals. *Angew. Chem. Int. Ed.* **2012**, *51*, 2564–2601. [CrossRef]
8. Gan, L.; Lyu, L.; Shen, T.; Wang, S. Sulfonated lignin-derived ordered mesoporous carbon with highly selective and recyclable catalysis for the conversion of fructose into 5-hydroxymethylfurfural. *Appl. Catal. A Gen.* **2019**, *574*, 132–143. [CrossRef]
9. Yabushita, M.; Kobayashi, H.; Fukuoka, A. Catalytic transformation of cellulose into platform chemicals. *Appl. Catal. B Environ.* **2014**, *145*, 1–9. [CrossRef]
10. Marques, C.; Tarek, R.; Sara, M.; Brar, S.K. Chapter 12—Sorbitol Production From Biomass and Its Global Market. In *Platform Chemical Biorefinery*; Elsevier: Amsterdam, The Netherlands, 2016; pp. 217–227. [CrossRef]
11. Gallezot, P. Conversion of biomass to selected chemical products. *Chem. Soc. Rev.* **2012**, *41*, 1538–1558. [CrossRef]
12. Fukuoka, A.; Dhepe, P.L. Catalytic conversion of cellulose into sugar alcohols. *Angew. Chem. Int. Ed.* **2006**, *45*, 5161–5163. [CrossRef]

13. Novoselov, N.P.; Sashina, E.S.; Petrenko, V.E.; Zaborsky, M. Study of dissolution of cellulose in ionic liquids by computer modeling. *Fibre Chem.* **2007**, *39*, 153–158. [CrossRef]
14. Tolonen, L.K.; Bergenstråhle-Wohlert, M.; Sixta, H.; Wohlert, J. Solubility of Cellulose in Supercritical Water Studied by Molecular Dynamics Simulations. *J. Phys. Chem. B* **2015**, *119*, 4739–4748. [CrossRef]
15. Yu, Y.; Wu, H. Effect of ball milling on the hydrolysis of microcrystalline cellulose in hot-compressed water. *AIChE J.* **2011**, *57*, 793–800. [CrossRef]
16. Siankevich, S. *Conversion of Biomass into Value-Added Chemicals*; EPFL: Lausanne, Switzerland, 2016.
17. Wu, Y.; Fu, Z.; Yin, D.; Xu, Q.; Liu, F.; Lu, C.; Mao, L. Microwave-assisted hydrolysis of crystalline cellulose catalyzed by biomass char sulfonic acids. *Green Chem.* **2010**, *12*, 696–700. [CrossRef]
18. Gitifar, V.; Eslamloueyan, R.; Sarshar, M. Experimental study and neural network modeling of sugarcane bagasse pretreatment with H_2SO_4 and O_3 for cellulosic material conversion to sugar. *Bioresour. Technol.* **2013**, *148*, 47–52. [CrossRef]
19. Huber, G.W.; Iborra, S.; Corma, A. Synthesis of transportation fuels from biomass: Chemistry, catalysts, and engineering. *Chem. Rev.* **2006**, *106*, 4044–4098. [CrossRef] [PubMed]
20. Zhang, Y.H.P.; Lynd, L.R. Toward an aggregated understanding of enzymatic hydrolysis of cellulose: Noncomplexed cellulase systems. *Biotechnol. Bioeng.* **2004**, *88*, 797–824. [CrossRef]
21. Zhou, C.H.; Xia, X.; Lin, C.X.; Tong, D.S.; Beltramini, J. Catalytic conversion of lignocellulosic biomass to fine chemicals and fuels. *Chem. Soc. Rev.* **2011**, *40*, 5588–5617. [CrossRef]
22. Suganuma, S.; Nakajima, K.; Kitano, M.; Yamaguchi, D.; Kato, H.; Hayashi, S.; Hara, M. Synthesis and acid catalysis of cellulose-derived carbon-based solid acid. *Solid State Sci.* **2010**, *12*, 1029–1034. [CrossRef]
23. Guarín, C.; Gavilà, L.; Constantí, M.; Medina, F. Impact of cellulose treatment with hydrotalcites in hydrothermal catalytic conversion. *Chem. Eng. Sci.* **2018**, *179*, 83–91. [CrossRef]
24. Huang, Y.B.; Fu, Y. Hydrolysis of cellulose to glucose by solid acid catalysts. *Green Chem.* **2013**, *15*, 1095–1111. [CrossRef]
25. Onda, A.; Ochi, T.; Yanagisawa, K. Hydrolysis of cellulose selectively into glucose over sulfonated activated-carbon catalyst under hydrothermal conditions. *Top. Catal.* **2009**, *52*, 801–807. [CrossRef]
26. Carlier, S.; Hermans, S. Highly Efficient and Recyclable Catalysts for Cellobiose Hydrolysis: Systematic Comparison of Carbon Nanomaterials Functionalized With Benzyl Sulfonic Acids. *Front. Chem.* **2020**, *8*, 347. [CrossRef] [PubMed]
27. Hoffer, B.W.; Crezee, E.; Mooijman, P.R.M.; Van Langeveld, A.D.; Kapteijn, F.; Moulijn, J.A. Carbon supported Ru catalysts as promising alternative for Raney-type Ni in the selective hydrogenation of D-glucose. *Catal. Today* **2003**, *79–80*, 35–41. [CrossRef]
28. Zhang, X.; Durndell, L.J.; Isaacs, M.A.; Parlett, C.M.A.; Lee, A.F.; Wilson, K. Platinum-Catalyzed aqueous-Phase hydrogenation of d-Glucose to d-Sorbitol. *ACS Catal.* **2016**, *6*, 7409–7417. [CrossRef]
29. Romero, A.; Alonso, E.; Sastre, Á.; Nieto-Márquez, A. Conversion of biomass into sorbitol: Cellulose hydrolysis on MCM-48 and d-Glucose hydrogenation on Ru/MCM-48. *Microporous Mesoporous Mater.* **2016**, *224*, 1–8. [CrossRef]
30. Wang, H.; Lv, J.; Zhu, X.; Liu, X.; Han, J.; Ge, Q. Efficient Hydrolytic Hydrogenation of Cellulose on Mesoporous HZSM-5 Supported Ru Catalysts. *Top. Catal.* **2015**, *58*, 623–632. [CrossRef]
31. Zhu, W.; Yang, H.; Chen, J.; Chen, C.; Guo, L.; Gan, H.; Zhao, X.; Hou, Z. Efficient hydrogenolysis of cellulose into sorbitol catalyzed by a bifunctional catalyst. *Green Chem.* **2014**, *16*, 1534. [CrossRef]
32. Chen, J.; Wang, S.; Huang, J.; Chen, L.; Ma, L.; Huang, X. Conversion of cellulose and cellobiose into sorbitol catalyzed by ruthenium supported on a polyoxometalate/metal-organic framework hybrid. *ChemSusChem* **2013**, *6*, 1545–1555. [CrossRef]
33. Deng, W.; Liu, M.; Tan, X.; Zhang, Q.; Wang, Y. Conversion of cellobiose into sorbitol in neutral water medium over carbon nanotube-supported ruthenium catalysts. *J. Catal.* **2010**, *271*, 22–32. [CrossRef]
34. Li, Z.; Liu, Y.; Liu, C.; Wu, S.; Wei, W. Direct conversion of cellulose into sorbitol catalyzed by a bifunctional catalyst. *Bioresour. Technol.* **2019**, *274*, 190–197. [CrossRef] [PubMed]
35. Hausoul, P.J.C.; Beine, A.K.; Neghadar, L.; Palkovits, R. Kinetics study of the Ru/C-catalysed hydrogenolysis of polyols-insight into the interactions with the metal surface. *Catal. Sci. Technol.* **2017**, *7*, 56–63. [CrossRef]
36. Van de Vyver, S.; Geboers, J.; Dusselier, M.; Schepers, H.; Vosch, T.; Zhang, L.; Van Tendeloo, G.; Jacobs, P.A.; Sels, B.F. Selective bifunctional catalytic conversion of cellulose over reshaped Ni particles at the tip of carbon nanofibers. *ChemSusChem* **2010**, *3*, 698–701. [CrossRef] [PubMed]
37. Kolpin, A.; Jones, G.; Jones, S.; Zheng, W.; Cookson, J.; York, A.P.E.; Collier, P.J.; Tsang, S.C.E. Quantitative Differences in Sulfur Poisoning Phenomena over Ruthenium and Palladium: An Attempt to Deconvolute Geometric and Electronic Poisoning Effects Using Model Catalysts. *ACS Catal.* **2017**, *7*, 592–605. [CrossRef]
38. Dreher, M.; Steib, M.; Nachtegaal, M.; Wambach, J.; Vogel, F. On-stream regeneration of a sulfur-poisoned ruthenium-carbon catalyst under hydrothermal gasification conditions. *ChemCatChem.* **2014**, *6*, 626–633. [CrossRef]
39. Li, Z.Q.; Lu, C.J.; Xia, Z.P.; Zhou, Y.; Luo, Z. X-ray diffraction patterns of graphite and turbostratic carbon. *Carbon N. Y.* **2007**, *45*, 1686–1695. [CrossRef]
40. Bloh, J.Z.; Dillert, R.; Bahnemann, D.W. Ruthenium-modified zinc oxide, a highly active vis-photocatalyst: The nature and reactivity of photoactive centres. *Phys. Chem. Chem. Phys.* **2014**, *16*, 5833–5845. [CrossRef]
41. Sassoye, C.; Muller, G.; Debecker, D.P.; Karelovic, A.; Cassaignon, S.; Pizarro, C.; Ruiz, P.; Sanchez, C. A sustainable aqueous route to highly stable suspensions of monodispersed nano ruthenia. *Green Chem.* **2011**, *13*, 3230–3237. [CrossRef]

42. Zada, B.; Chen, M.; Chen, C.; Yan, L.; Xu, Q.; Li, W.; Guo, Q.; Fu, Y. Recent advances in catalytic production of sugar alcohols and their applications. *Sci. China Chem.* **2017**, *60*, 853–869. [CrossRef]
43. Chaturvedi, V.; Verma, P. An overview of key pretreatment processes employed for bioconversion of lignocellulosic biomass into biofuels and value added products. *3 Biotech.* **2013**, *3*, 415–431. [CrossRef]
44. Mood, S.H.; Golfeshan, A.H.; Tabatabaei, M.; Jouzani, G.S.; Najafi, G.H.; Gholami, M.; Ardjmand, M. Lignocellulosic biomass to bioethanol, a comprehensive review with a focus on pretreatment. *Renew. Sustain. Energy Rev.* **2013**, *27*, 77–93. [CrossRef]
45. Liao, Y.; de Beeck, B.O.; Thielemans, K.; Ennaert, T.; Snelders, J.; Dusselier, M.; Courtin, C.M.; Sels, B.F. The role of pretreatment in the catalytic valorization of cellulose. *Mol. Catal.* **2020**, *487*, 110883. [CrossRef]
46. Hausoul, P.J.C.; Negahdar, L.; Schute, K.; Palkovits, R. Unravelling the Ru-Catalyzed Hydrogenolysis of Biomass-Based Polyols under Neutral and Acidic Conditions. *ChemSusChem* **2015**, *8*, 3323–3330. [CrossRef] [PubMed]
47. Luo, C.; Wang, S.; Liu, H. Cellulose conversion into polyols catalyzed by reversibly formed acids and supported ruthenium clusters in hot water. *Angew. Chem. Int. Ed.* **2007**, *46*, 7636–7639. [CrossRef]
48. Kobayashi, H.; Matsuhashi, H.; Komanoya, T.; Hara, K.; Fukuoka, A. Transfer hydrogenation of cellulose to sugar alcohols over supported ruthenium catalysts. *Chem. Commun.* **2011**, *47*, 2366–2368. [CrossRef]
49. Almohalla, M.; Rodríguez-Ramos, I.; Ribeiro, L.S.; Órfão, J.J.M.; Pereira, M.F.R.; Guerrero-Ruiz, A. Cooperative action of heteropolyacids and carbon supported Ru catalysts for the conversion of cellulose. *Catal. Today* **2018**, *301*, 65–71. [CrossRef]
50. Han, J.W.; Lee, H. Direct conversion of cellulose into sorbitol using dual-functionalized catalysts in neutral aqueous solution. *Catal. Commun.* **2012**, *19*, 115–118. [CrossRef]
51. Lazaridis, P.A.; Karakoulia, S.A.; Teodorescu, C.; Apostol, N.; Macovei, D.; Panteli, A.; Delimitis, A.; Coman, S.M.; Parvulescu, V.I.; Triantafyllidis, K.S. High hexitols selectivity in cellulose hydrolytic hydrogenation over platinum (Pt) vs. ruthenium (Ru) catalysts supported on micro/mesoporous carbon. *Appl. Catal. B Environ.* **2017**, *214*, 1–14. [CrossRef]
52. Negoi, A.; Triantafyllidis, K.; Parvulescu, V.I.; Coman, S.M. The hydrolytic hydrogenation of cellulose to sorbitol over M (Ru, Ir, Pd, Rh)-BEA-zeolite catalysts. *Catal. Today* **2014**, *223*, 122–128. [CrossRef]
53. Zhang, G.; Chen, T.; Zhang, Y.; Liu, T.; Wang, G. Effective Conversion of Cellulose to Sorbitol Catalyzed by Mesoporous Carbon Supported Ruthenium Combined with Zirconium Phosphate. *Catal. Lett.* **2020**, *150*, 2294–2303. [CrossRef]
54. Stellwagen, D.R.; Van Der Klis, F.; Van Es, D.S.; De Jong, K.P.; Bitter, J.H. Functionalized carbon nanofibers as solid-acid catalysts for transesterification. *ChemSusChem* **2013**, *6*, 1668–1672. [CrossRef] [PubMed]
55. Boehm, H.-P.; Diehl, E.; Heck, W.; Sappok, R. Surface Oxides of Carbon. *Angew. Chem. Int. Ed. Engl.* **1964**, *3*, 669–677. [CrossRef]
56. Goertzen, S.L.; Thériault, K.D.; Oickle, A.M.; Tarasuk, A.C.; Andreas, H.A. Standardization of the Boehm titration. Part I. CO2 expulsion and endpoint determination. *Carbon N. Y.* **2010**, *48*, 1252–1261. [CrossRef]